



ELSEVIER

Available online at [www.sciencedirect.com](http://www.sciencedirect.com)

SCIENCE @ DIRECT®

Journal of Crystal Growth 272 (2004) 526–530

JOURNAL OF **CRYSTAL GROWTH**

[www.elsevier.com/locate/jcrysgro](http://www.elsevier.com/locate/jcrysgro)

# Metalorganic vapor-phase epitaxy of room-temperature, low-threshold InGaAs/AlInAs quantum cascade lasers

D. Bour<sup>a,\*</sup>, M. Troccoli<sup>b</sup>, F. Capasso<sup>b</sup>, S. Corzine<sup>a</sup>, A. Tandon<sup>a</sup>, D. Mars<sup>a</sup>, G. Höfler<sup>a</sup>

<sup>a</sup>Agilent Laboratories, Photonics and Electronics Research Laboratory, 3500 Deer Creek Road, Palo Alto, CA 94304, USA

<sup>b</sup>Harvard University, Division of Engineering and Applied Science, Cruft Laboratory 310, 19 Oxford Street, Cambridge, MA 02139, USA

Available online 7 October 2004

## Abstract

We have grown 30-stage AlInAs-GaInAs quantum cascade laser structures by low-pressure metalorganic vapor-phase epitaxy (MOVPE). The growth rate for the active region was set very low (0.1 nm/s), and growth stops were employed at all interfaces. The devices were operated pulsed at room temperature, with a threshold current density of 2.8 kA/cm<sup>2</sup>, a lasing wavelength of 7.6 μm, and a peak power of 150 mW. CW operation was achieved up to a temperature of 180 K. These characteristics compare favorably with MBE-grown QC lasers of similar structure.

© 2004 Elsevier B.V. All rights reserved.

**Keywords:** A3. Metalorganic vapor phase epitaxy; A3. Quantum wells; B2. Semiconducting III–V materials; B3. Heterojunction semiconductor devices; B3. Laser diodes

## 1. Introduction

Since their initial invention and demonstration, nearly all quantum cascade lasers (QCLs) have been fabricated using molecular beam epitaxy (MBE) [1–4]. The primary advantages of MBE include excellent composition and thickness control, along with the ease of forming atomically abrupt interfaces. Quantum cascade laser growth

is especially demanding in this regard, because the most critical layers included in the heterostructure are extremely thin (1–2 nm). However, the quality of quantum cascade (QC) heterostructures deposited by metalorganic vapor-phase epitaxy (MOVPE) may approach that of MBE, so long as the proper growth parameters are employed; and in this manner MOVPE-grown QCLs have been recently reported [5,6].

The viability of MOVPE for production of QCLs deserves further consideration; and at this early stage we anticipate significant improvements in performance. While the outstanding control

\*Corresponding author. Tel.: +16504855485; fax: +16504853341.

E-mail address: [dave\\_bour@agilent.com](mailto:dave_bour@agilent.com) (D. Bour).

afforded by MBE makes it ideally suited to the growth of QCLs, MOVPE may still offer some advantages over MBE. For example, eliminating oxygen contamination from aluminum-containing alloys is more straightforward by MOVPE. Likewise, higher growth rates are possible, and growth of thick InP cladding layers is routine. On the other hand, the requisite control of interface abruptness is more challenging by MOVPE, and the carbon background of AlGaAs alloys may translate into shorter electron coherence length in the QCL stages. These tradeoffs between MBE and MOVPE must still be evaluated.

Here we describe the growth and performance of a 30-stage AlInAs/GaInAs/InP QC laser grown by low-pressure MOVPE. This QCL replicates the MBE-grown structure described by Gmachl et al. for 8  $\mu\text{m}$  wavelength [4]. By setting the growth rate very low and incorporating growth stops at all active region interfaces, QC lasers with low-threshold current density were realized, with pulsed  $J_{\text{th}} = 0.8 \text{ kA/cm}^2$  at 80 K and  $2.8 \text{ kA/cm}^2$

at 300 K and a lasing wavelength of 7.6  $\mu\text{m}$  at room temperature. These thresholds compare favorably with MBE-grown QC lasers of similar structure, suggesting that MOVPE can be effective for the production of these sophisticated structures.

## 2. Experimental procedure

The QCL structure is shown in Fig. 1. It incorporates a three quantum well, vertical-transition active region designed for 8  $\mu\text{m}$  emission wavelength, as described by Gmachl et al. [4], along with InP cladding layers. The designed thickness for each of the lattice-matched AlInAs and GaInAs layers comprised in a single stage are 3.8/2.1/1.2/6.5/1.2/5.3/2.3/4.0/1.1/3.6/1.2/3.2/1.2/3.0/1.6/3.0 nm (starting from the AlInAs injection barrier; the underlined layers are doped with silicon to  $2 \times 10^{17} \text{ cm}^{-3}$ ).

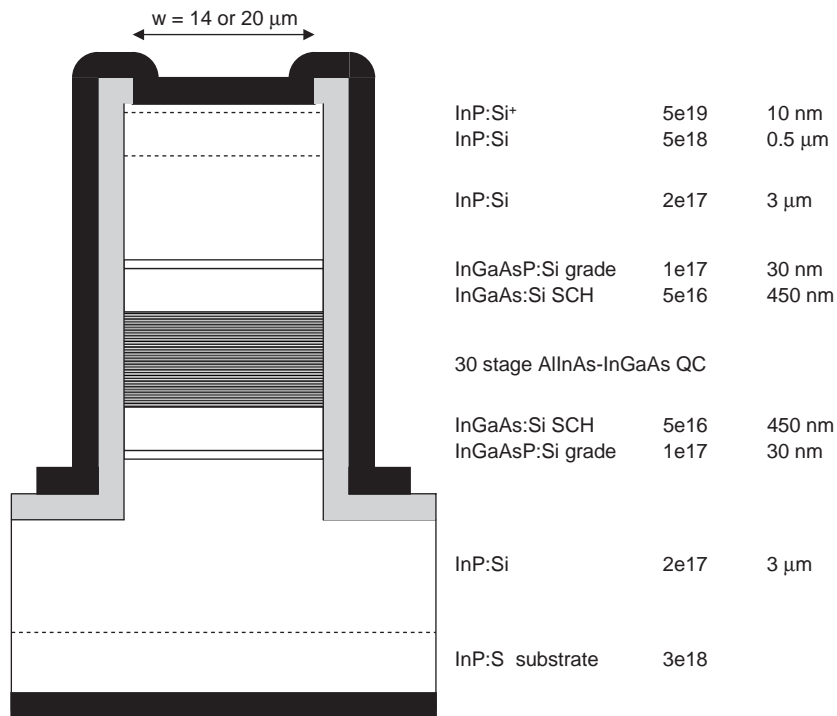


Fig. 1. Structure of MOVPE-grown QCL, showing layer thicknesses and doping.

Growth was by conventional, low-pressure (76 Torr) MOVPE. Our Thomas Swan MOVPE reactor incorporates a pressure-balanced switching manifold and a close-spaced showerhead injector. Similar to the conditions employed by Roberts et al. [5], the growth rate for the QC active region was set very low (0.1 nm/s), and growth stops were employed at all interfaces. The remainder of the structure was grown at roughly 5 times this rate. Precursors include trimethylindium, triethylgallium (for the slow-grown QC structure only), trimethylgallium (for the InGaAs separate confinement heterostructure), trimethylaluminum, arsine, phosphine, and disilane (0.01% in H<sub>2</sub>) for *n*-type doping. The samples were grown at a temperature of 650 °C (real temperature, calibrated by the eutectic temperature of Al:Si) on (001)-oriented InP:S ( $n = 3 \times 10^{18} \text{ cm}^{-3}$ ) substrates. To avoid excessive free-carrier loss associated with the high doping in the substrate, a relatively thick (3 μm) low *n*-type InP:Si ( $n = 2 \times 10^{17} \text{ cm}^{-3}$ ) cladding layer was grown before the InGaAs separate confinement heterostructure (SCH) and QC active region. Likewise, the InP upper cladding layer is of similar thickness and doping, to minimize the loss arising from the plasmon guiding layer (500 nm InP:Si with  $n = 5 \times 10^{18} \text{ cm}^{-3}$ ) and metal contact. Based on TM-mode profile simulations, 450 nm InGaAs SCH layers ( $n = 5 \times 10^{16} \text{ cm}^{-3}$ ) are placed symmetrically about the active region. To reduce the series resistance, the interfaces between the InGaAs SCH and the InP cladding layers comprise 30 nm step-graded InGaAsP. The V:III ratio was approximately 300 for the QC active region, 200 for the InP cladding layers, and 80 for the InGaAs SCH layers.

The measured (004) X-ray diffraction spectra of the QC laser wafer is shown in Fig. 2, in comparison to the simulated spectra (bottom). Satellite reflections are clearly visible, indicating the presence of a periodic structure. The spacing of the satellites indicates a periodicity of about 42 nm, corresponding to the thickness of each QC stage. This is slightly thinner than the designed stage thickness of 44 nm. This difference could be an indication of a systematic error, where each layer forming the QC stack is about 5% too thin,

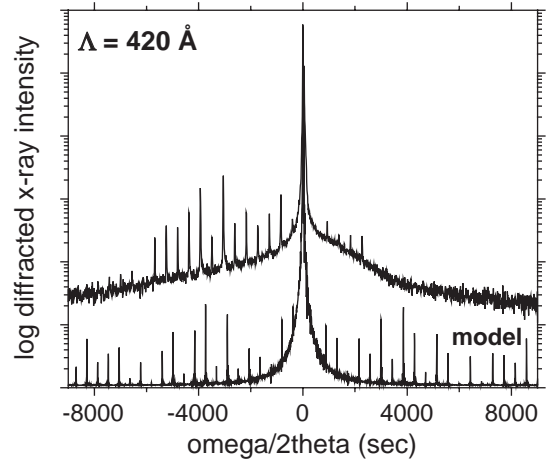


Fig. 2. Comparison of measured (top) and simulated (bottom) (004) X-ray diffraction from MOVPE-grown QCL.

which would also be consistent with the observed blue-shifted wavelength with respect to the original design (7.6 vs. 8.1 μm).

After growth, the wafers were processed into deep-etched ridge waveguide lasers, of widths 14 or 20 μm. The narrower stripes were used for the highest temperature continuous wave operation given the lower current needed to reach threshold and therefore the lower power to be dissipated in the device. The lasers were cleaved into bars of 2 mm cavity length, soldered epitaxial-side-up to metal heat sinks, wire bonded, then mounted in a liquid-nitrogen-flow cryostat for electrical and optical characterization. The gold metal top-contact is only 350 nm thick for comparison with the original results in Ref. [4], unlike the most recent high-performance MBE-grown devices with very thick (~5 μm) gold contacts [7].

### 3. Results and discussion

The power–current (*L–I*) and voltage–current (*V–I*) characteristics for a wide stripe (20 μm × 2 mm) laser are shown in Fig. 3, for pulsed operation at heat-sink temperatures of 80 and 300 K. The lasers were driven with a current pulse of width 100 ns, at a repetition rate of 5 kHz. The threshold current density is 0.8 kA/cm<sup>2</sup> at

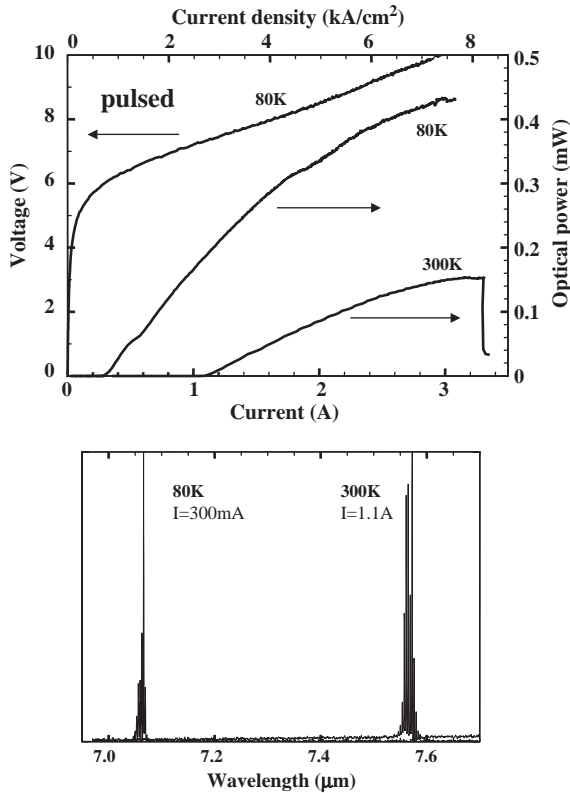


Fig. 3. Top: Power–current and voltage–current characteristics for pulsed operation at 80 and 300 K, of 20 μm × 2 mm MOVPE-grown QCL. Bottom: Corresponding spectra at 80 and 300 K.

80 K, and 2.8 kA/cm<sup>2</sup> at 300 K. The peak power is about 440 and 150 mW at 80 and 300 K, respectively. The emission wavelength varies from 7.1 μm at 80 K to 7.6 μm at room temperature, as shown by the spectra inset in Fig. 3.

We also prepared samples with AlInAs replacing the InP for the upper cladding layer. In this case, the InGaAs SCH was made asymmetric, again with a structure like those reported by Gmachl et al. to compensate for the difference in the refractive index between InP and AlInAs [4]. These samples with AlInAs upper cladding exhibit pulsed performance characteristics similar to those with InP upper cladding, however their cw characteristics are inferior, presumably due to the relatively poor thermal conductivity of AlInAs.

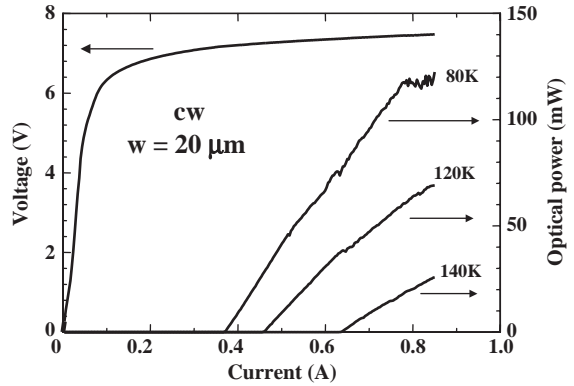


Fig. 4. cw power–current and voltage–current characteristics at various heat-sink temperatures, for wide-stripe ( $w = 20 \mu\text{m}$ ) MOVPE-grown QCLs of length  $L = 2 \text{ mm}$ .

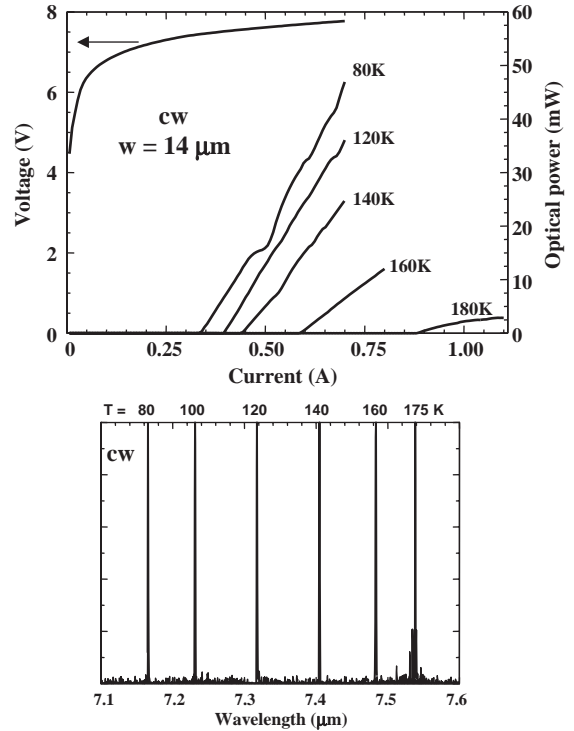


Fig. 5. cw power–current and voltage–current characteristics at various heat-sink temperatures, for narrow-stripe ( $w = 14 \mu\text{m}$ ) MOVPE-grown QCLs of length  $L = 2 \text{ mm}$ . Bottom right shows cw emission spectra at several temperatures.

The cw operating characteristics of these wide-stripe QC lasers are shown in Fig. 4. They are capable of cw operation at temperatures as high as

140 K, and at 80 K the maximum average power is about 120 mW. The lasers with a narrower stripe ( $14\ \mu\text{m} \times 2\ \text{mm}$ ) were also tested under continuous injection conditions, as shown by the  $L$ – $I$ – $V$  characteristics in Fig. 5. For the narrower stripe the maximum cw operation temperature is 180 K. The cw threshold current density variation with heat-sink temperature can be described by  $J = J_0 \exp(T/T_0)$ , with a characteristic temperature  $T_0 \sim 105\ \text{K}$ . The spectra for cw operation of the narrow-stripe lasers are also shown in Fig. 5, for temperatures 80–175 K. For cw, substrate-side-down operation of these  $14\ \mu\text{m}$  wide stripes in the temperature range 80–180 K, the coefficient of wavelength change with respect to heat-sink temperature was measured to be approximately 4 nm/K.

#### 4. Conclusions

We have grown 30-stage AlInAs-GaInAs QCL structures by low-pressure MOVPE, in a reactor incorporating a pressure-balanced switching manifold and a close-spaced showerhead injector. The growth rate for the active region was set very low (0.1 nm/s), and growth stops were employed at all interfaces. The ridge devices of length 2 mm and width  $20\ \mu\text{m}$  were operated pulsed at room temperature, with a threshold current density of  $2.8\ \text{kA/cm}^2$ , a lasing wavelength  $7.6\ \mu\text{m}$ , and a

peak power of 150 mW. For narrower stripes ( $14\ \mu\text{m}$ ) cw operation was achieved at a maximum temperature of 180 K. These characteristics compare favorably with MBE-grown QC lasers of similar structure, indicating that MOVPE is a viable technique for the fabrication of these challenging structures.

#### References

- [1] J. Faist, F. Capasso, D.L. Sivco, C. Sirtori, A.L. Hutchinson, A.Y. Cho, *Science* 264 (1994) 553.
- [2] J. Faist, F. Capasso, C. Sirtori, D.L. Sivco, A.Y. Cho, Quantum cascade lasers, in: H.C. Liu, F. Capasso (Eds.), *Intersubband Transitions in Quantum Wells: Physics and Device Applications II*, Semiconductors and Semimetals, Vol. 66, Academic Press, New York, 2000 (Chapter 1).
- [3] F. Capasso, R. Paiella, R. Martini, R. Colombelli, C. Gmachl, T.L. Myers, M.S. Taubman, R.M. Williams, C.G. Bethea, K. Unterrainer, H.Y. Hwang, D.L. Sivco, A.Y. Cho, A.M. Sergent, H.C. Liu, E.A. Whittaker, *IEEE J. Quantum Electron.* 38 (2002) 511.
- [4] C. Gmachl, A. Tredicucci, F. Capasso, A.L. Hutchinson, D.L. Sivco, J.N. Baillergeon, A.Y. Cho, *Appl. Phys. Lett.* 72 (1998) 3130–3132.
- [5] J.S. Roberts, R.P. Green, L.R. Wilson, E.A. Zibik, D.G. Revin, J.W. Cockburn, R.J. Airey, *Appl. Phys. Lett.* 82 (2003) 4221.
- [6] R.P. Green, A. Krysa, J.S. Roberts, D.G. Revin, L.R. Wilson, E.A. Zibik, W.H. Ng, J.W. Cockburn, *Appl. Phys. Lett.* 83 (2003) 1921–1923.
- [7] J.S. Yu, A. Evans, J. David, L. Doris, S. Slivken, M. Razhegi, *IEEE Photonics Technol. Lett.* 16 (2004) 747.